



PRIMA: Multi-Image Vision-Language Models for Reasoning Segmentation

Muntasir Wahed^{1*} Kiet A. Nguyen^{1*} Adheesh Juvekar¹ Xinzhuo Li¹
 Xiaona Zhou¹ Vedant Shah¹ Tianjiao Yu¹ Pinar Yanardag² Ismini Lourentzou¹
¹University of Illinois Urbana - Champaign ²Virginia Tech

{mwahed2, kietan2, adheesh2, xinzhuo4, xiaonaz2, vrshah4, ty41, lourent2}@illinois.edu, {pinary}@vt.edu

<https://plan-lab.github.io/prima>

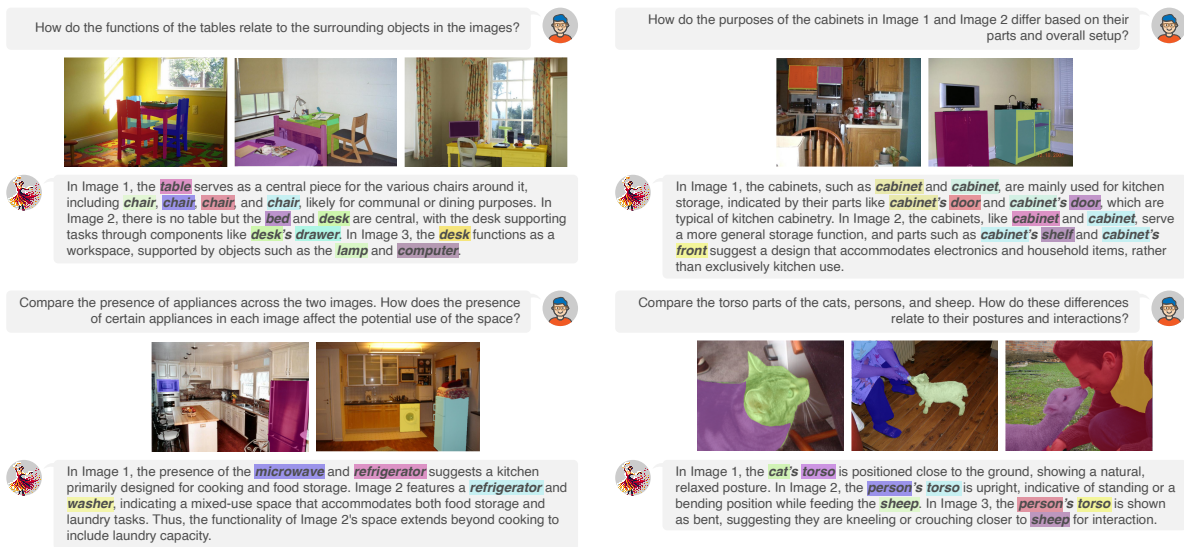


Figure 1. We introduce the new task of multi-image pixel-grounded reasoning segmentation at both object and part levels. To support this task, we curate M^4SEG , a benchmark providing question-answer pairs alongside image sets annotated with object and part segmentation masks. Additionally, we propose PRIMA, a model trained on M^4SEG , designed to efficiently identify and compare object functionalities and contextual relationships across scenes.

Abstract

Despite significant advancements in Large Vision-Language Models (LVLMs), existing pixel-grounding models operate on single-image settings, limiting their ability to perform detailed, fine-grained comparisons across multiple images. Conversely, current multi-image understanding models lack pixel-level grounding. Our work addresses this gap by introducing the task of multi-image pixel-grounded reasoning segmentation, and PRIMA, a novel LVLM that integrates pixel-level grounding with robust multi-image reasoning capabilities to produce contextually rich, pixel-grounded explanations. Central to PRIMA is an efficient vision module that queries fine-grained visual representations across multiple images,

reducing TFLOPs by 25.3%. To support training and evaluation, we curate M^4SEG , a new reasoning segmentation benchmark consisting of $\sim 224K$ question-answer pairs that require fine-grained visual understanding across multiple images. Experimental results demonstrate PRIMA outperforms state-of-the-art baselines.

1. Introduction

Large Vision-Language Models (LVLMs) have demonstrated remarkable success in reasoning and perception tasks, due to their ability to jointly understand and process visual and textual information. LVLMs leverage large-scale multimodal data that leads to improved performance on var-

* Equal Contribution.
 Preprint. Work in Progress.

ious downstream tasks, *i.e.*, question answering [29], image captioning [26, 44], object detection [8], *etc.* The synergy between vision and language has also paved the way for more sophisticated image understanding capabilities, including spatial reasoning [7], semantic segmentation [23], reasoning segmentation [22], *etc.* These advancements have enabled precise pixel-level grounding and reasoning referring to objects within an image, which improves both the quality and the explainability of the generated response.

Despite these advances in single-image visual perception, fine-grained comparative analysis across images remains an open challenge, especially in scenarios where understanding subtle differences or similarities between images is crucial. Such multi-image understanding is fundamentally different from single-image understanding because different tasks would require a joint understanding of different visual elements across images. For example, as shown in Figure 1, depending on the nature of the task, the model must identify varied fine-grained differences in visual scenes, such as the presence and functions of objects, compare objects in terms of spatial arrangements, and ground part-level functionalities across diverse contexts.

The ability to analyze multi-image contexts allows models to discern specific visual features that may differ across instances of the same object, or that serve as distinguishing features between different objects, enabling a wide range of applications, from detailed visual analysis (*e.g.*, medical imaging) to tasks like e-commerce, where comparing product details is crucial. Furthermore, fine-grained cross-image comparisons with pixel-level grounding can also enhance the interpretability of LVLMs, offering localized visual explanations for why certain visual elements are prioritized.

Existing works on LVLm-based pixel grounding and reasoning, *e.g.*, LISA [22] or GLaMM [37], have focused on aligning textual descriptions with specific regions or pixels within an image. However, they primarily focus on single-image scenarios, lacking the ability to perform coherent multi-image reasoning. On the other hand, recent works such as SparklesChat [16] and VPG-C [25] have explored multi-image understanding by facilitating dialogue systems and visual perception across multiple images. These approaches highlight the importance of cross-image comparison and dialogue-based understanding but lack the detailed pixel-level grounding essential for fine-grained multi-image visual analysis.

To bridge the research gap between multi-image understanding and pixel-level grounding, in this work, we introduce the new task of *multi-image pixel-grounded reasoning segmentation*, where given a comparative free-form question involving two or more images, a model must produce a natural language response accompanied by pixel-level grounding of the relevant objects and parts. To our knowledge, this is the first work to formalize this com-

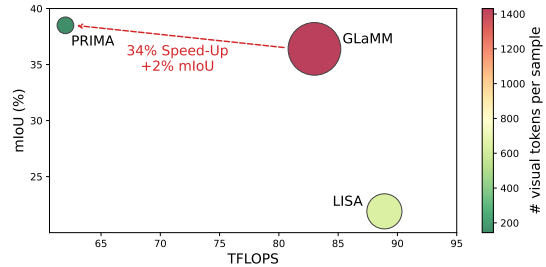


Figure 2. **Computational Efficiency Comparison.** TFLOPs vs. mIoU performance, with marker size representing # tokens/image. PRIMA outperforms SoTA baselines on M⁴SEG while using only 57.9 tokens on average, which is approximately 4 times fewer tokens than LISA (256) and nearly 10 times fewer tokens than GLaMM (576), reducing TFLOPs over GLaMM by 25.3%.

bined fine-grained reasoning and grounding task. To facilitate evaluation in this novel task, we introduce M⁴SEG, a new benchmark consisting of ~224K comparative questions that require simultaneous reasoning across multiple images along with corresponding answers grounded on the objects and part information. M⁴SEG contains 115 unique objects and 251 unique parts, with each question-answer pair featuring multiple cross-image target objects and part segmentation masks, making it a challenging benchmark for multi-image pixel-grounded reasoning segmentation. Additionally, we propose PRIMA, the first **P**ixel-g**R**ounded **M**ulti-**I**mage **S**eg**M**entation **R**easoning **V**ision-**L**anguage **M**odel for this task. PRIMA employs an instruction-guided multi-image adaptation module to reason across multiple images with fine-grained grounding. Experimental results demonstrate strong performance and computational efficiency compared to state-of-the-art baselines (Figure 2). In summary, the contributions of this work are as follows:

- We propose the novel task of multi-image pixel-grounded reasoning segmentation, which necessitates fine-grained comparison and contextual understanding across multiple images at the pixel level, requiring models to produce responses grounded in specific objects and parts.
- We introduce M⁴SEG, a new challenging benchmark with over 224K multi-image QA pairs, annotated with multiple object and part segmentation masks to enable and evaluate pixel-grounded multi-image visual understanding.
- We propose PRIMA, a vision-language model specifically designed for this new task. Unlike existing models, PRIMA excels in generating natural language responses accompanied by contextually grounded segmentations across multiple images. PRIMA is optimized for computational efficiency by incorporating a cross-modal attention mechanism, which enables instruction-guided alignment of relevant visual features across images, reducing overhead while maintaining high accuracy in pixel-level reasoning. Extensive experiments demonstrate PRIMA’s performance and efficiency against strong baselines.

2. Related Work

LVLMs have made significant strides in reasoning, segmentation, and multimodal understanding. However, as summarized in Table 1, existing models either generate ungrounded responses or perform single-image pixel-grounding, restricting their utility for fine-grained multi-image visual reasoning tasks. Our work aims to address this gap with a new multi-image pixel-grounding reasoning segmentation task that supports detailed, cross-image comparisons and contextual reasoning for objects and parts.

2.1. Large Vision Language Models (LVLMs)

Recent advancements have broadened the research focus from traditional text-only language models to models integrating both visual and textual information, thereby enhancing multimodal reasoning capabilities. Models like LLaVA [29], BLIP-2 [26], and Flamingo [1] have explored combining visual and language modalities through various integration techniques, from embedding visual features into the LLM input space to deeper fusion within intermediate layers. Other developments, such as Kosmos-2 [33], Shikra [5], and Ferret [55], have introduced object localization tasks to enhance visual comprehension, while Emu [42], CogVLM [45], and DreamLLM [14] have focused on incorporating visual generation capabilities.

Building on this foundation, various methods have emerged to further enhance LVLm reasoning. VICL [67] aligns relevant visual examples with text prompts to improve prediction accuracy without parameter updates, while ViGoR [52] enhances visual grounding through fine-grained reward modeling, leveraging both human feedback and automated visual perception tools for better alignment between generated text and image content. STIC [13] employs a two-stage self-training process by generating preference datasets from unlabeled images and fine-tuning the model on this data, enhancing comprehension without the need for pre-labeled inputs. Multimodal-CoT [64] extends chain-of-thought prompting to multimodal inputs to improve logical coherence across modalities, while MVP [34] addresses hallucinations with a multi-view multi-path reasoning mechanism that selects accurate answers. However, these models primarily focus on high-level reasoning, unlike specialized segmentation approaches that improve the capabilities LVLms to perform pixel-level understanding.

2.2. LVLm-Based Multi-Image Understanding

Recent developments in LVLm-based multi-image understanding have introduced various methods aimed at enhancing fine-grained reasoning, cross-modal interactions, and multimodal dialogues. SparklesChat [16] and VPG-C [25] improve coherence across images in multimodal instruction-following tasks by integrating multiple images

	Dataset (Model, Venue)	Objects	Parts	Seg. Masks	Multi-Image
Image-level	AS-V2 (ASMv2, ECCV-24) [46]	✓	✗	✗	✗
	LVIS-Ground (Groma, ECCV-24) [30]	✓	✗	✗	✗
	MANTIS-INSTRUCT (MANTIS, CVPR-24) [18]	✓	✗	✗	✓
	MMRA (arXiv-24) [50]	✓	✓	✗	✓
	CompBench (NeurIPS-24) [20]	✓	✓	✗	✓
M4-Instruct (LLaVA-NeXT-Interleave, CVPR-24) [24]	✓	✓	✗	✓	
Pixel-level	FP-RefCOCO (SESAME, CVPR-24) [51]	✓	✗	✓	✗
	RecapD (RGPT, CVPR-24) [15]	✓	✗	✓	✗
	MUSE (PixellLM, CVPR-24) [39]	✓	✗	✓	✗
	LLM-Seg40K (LLM-Seg, CVPR-24) [43]	✓	✓	✓	✗
	MMR (M ² SA, under review ICLR-25) [3]	✓	✓	✓	✗
	MGSC (MGLMM, arXiv-23) [66]	✓	✓	✓	✗
	MRES-32M (UniRES, CVPR-24) [47]	✓	✓	✓	✗
	GranD (GLaMM, CVPR-24) [37]	✓	✓	✓	✗
	ReasonSeg (LISA, CVPR-24) [22]	✓	✓	✓	✗
	M ⁴ SEG (ours)	✓	✓	✓	✓

Table 1. **Comparison of existing benchmarks and models for Vision-Language Reasoning and Segmentation.** Each dataset/model is evaluated on reasoning capabilities, multi-image understanding, and its focus on object and part-level understanding. The first column differentiates datasets that provide pixel-level annotations, and conversely, models that can perform finer-grained reasoning, from those that operate primarily at an image level. Our proposed benchmark (M⁴SEG) and LVLm (PRIMA) uniquely offer multi-image pixel-grounded conversational reasoning capabilities at both object and part levels.

into dialogue at the word level and generating intermediate-layer guidance to enrich visual reasoning, respectively. CaD-VI [28] and Leopard [17] both enhance comprehension of relationships between images, with CaD-VI focusing on structured visual comparisons between image pairs and Leopard leveraging an adaptive high-resolution encoding module for text-rich, multi-image tasks. To address challenges in handling diverse modalities and long image sequences, methods such as MMMModal [68], LLaVA-NeXT-Interleave [24], and MANTIS [18] employ interleaving techniques to facilitate richer multi-modal reasoning. MMMModal aligns visual and audio data for complex, context-aware interactions, while LLaVA-NeXT-Interleave integrates images, videos, and 3D data to capture intricate visual relationships. In contrast, MANTIS uses interleaved text and images to develop co-reference, reasoning, and temporal understanding. mPLUG-Owl3 [54] and LongLLaVA [48] address long image-sequence understanding using cross-attention mechanisms and hybrid architectures to scale model performance for up to 1000 images. These approaches underscore the need for cross-image comparisons and dialogue-based understanding, but they lack the detailed pixel-level grounding required for fine-grained visual analysis.

2.3. LVLm-Based Pixel Grounding

In the pursuit of enabling LVLms to generate segmentation masks, several methods have been proposed to tackle challenges in pixel-level grounding. GPT4ROI [60], Ferret [56], Osprey [57] are multi-modal models that process images with bounded regions and text prompts, using techniques like spatial instruction tuning, hybrid region representations, mask-text tuning, and localized visual tokeniza-

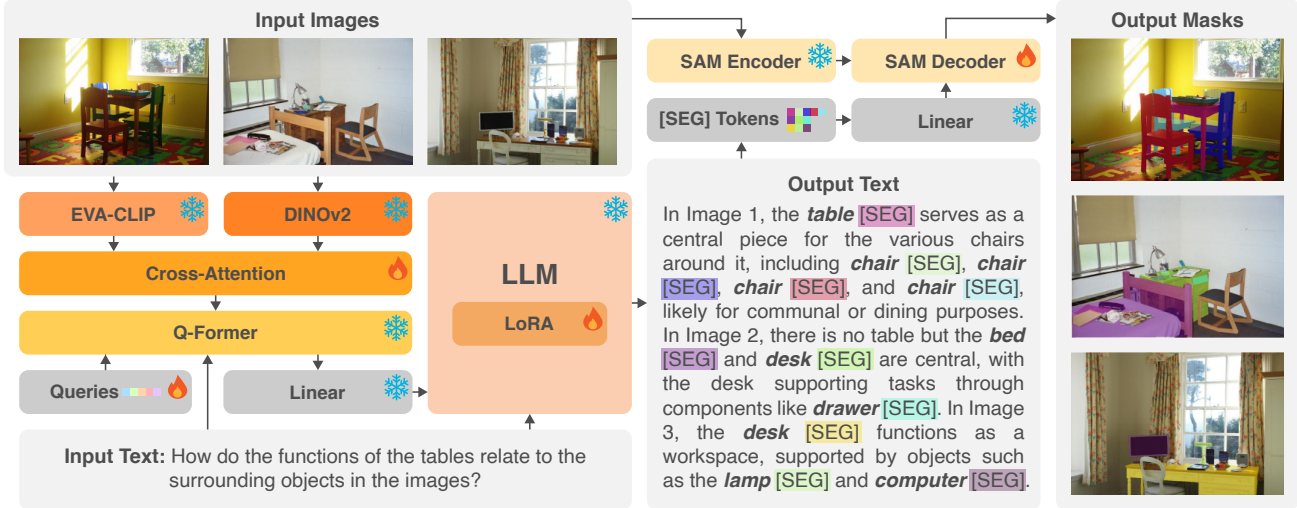


Figure 3. **Overview of the proposed PRIMA architecture.** PRIMA integrates a multi-image vision encoder that combines DINOv2 for dense semantic feature extraction and Q-Former’s selective query-based cross-attention to fuse relevant representations across images. The encoder outputs are mapped to a shared semantic space to facilitate precise pixel-level multi-image grounding. Leveraging a LoRA-finetuned language model and a SAM-based decoder, PRIMA dynamically generates segmentation masks corresponding to objects and parts referenced in natural language queries, supporting pixel-grounded reasoning in complex multi-image tasks.

tion to deliver precise, context-rich descriptions for detailed visual reasoning. On the other hand, BRAVE [19] and Mini-Gemini [27] enhance vision-language models by broadening visual encoding and integrating dual-resolution inputs, respectively, to improve holistic image understanding and reasoning-based text generation, though they do not address pixel-level segmentation.

Another line of research has significantly advanced segmentation grounding through multimodal models that blend language and vision, each with unique methods for generalization and precision. Models like PSALM [63], OMGLLaVA [61], NEXt-Chat [58], and GROUNDHOG [62] leverage mask decoders, bounding boxes, holistic segmentation, and pixel-level grounding to support complex segmentation across varied object localizations. LISA [22] pioneered referring segmentation by embedding a [SEG] token within the language model for targeted segmentation responses, later extended by LISA++ [53], which added instance segmentation and multi-turn dialogue. PixelLM [39] further refines precision with a lightweight decoder for multi-target segmentation. GLaMM [37] enhances flexibility by supporting both textual and visual prompts, enabling seamless multi-turn segmentation interactions. While these approaches significantly improved pixel-level visual grounding and reasoning segmentation, they primarily target single-image scenarios and lack the capability for coherent multi-image reasoning, specifically w.r.t. generating natural language responses grounded in multiple object and part segmentation masks across images. We propose PRIMA to address this critical gap and establish M⁴SEG as a new benchmark that supports training and eval-

uation for this new multi-image pixel-grounded reasoning segmentation task.

3. Method

3.1. Problem Definition

In multi-image pixel-grounded reasoning segmentation, we are given a natural language prompt \mathbf{T}_P and N_I images $\mathbf{I} = \{\mathbf{I}_1, \dots, \mathbf{I}_{N_I}\}$, where each image $\mathbf{I}_j \in \mathbb{R}^{3 \times H_j \times W_j}$ is of height H_j and width W_j . The objective is to generate a response that addresses the query by grounding relevant noun phrases in segmentation masks across the series of images. The resulting response includes sets of grounded segments $\mathbf{G} = \{\mathbf{G}_1, \dots, \mathbf{G}_{N_I}\}$, with each $\mathbf{G}_j = \{\mathbf{g}_{j1}, \dots, \mathbf{g}_{jG_j}\} \in \mathbb{R}^{G_j \times H_j \times W_j}$ containing G_j text groundings associated with image j . These groundings correspond to a set of segmentation masks \mathbf{M} : specifically, for image j , the groundings \mathbf{G}_j map to a set of binary masks $\mathbf{M}_j = \{\mathbf{m}_{j1}, \dots, \mathbf{m}_{jG_j}\} \in \{0, 1\}^{G_j \times H_j \times W_j}$, where a pixel in \mathbf{m}_{ji} is assigned the value 1 if it covers the visual element associated with grounding \mathbf{g}_{ji} in image j , and 0 otherwise. Each image may correspond to any number of masks, including zero, provided that there is at least one grounding in the response. In other words, $G_j \geq 0$ for any image j and $\sum_{j=1}^{N_I} G_j \geq 1$.

To accomplish this task, we propose PRIMA, a model that integrates an LVLM \mathcal{L} and a segmentation decoder \mathcal{S} . Here, the model response $\mathbf{T}_{\text{PRIMA}} = \mathcal{L}(\mathbf{T}_P, \mathbf{I})$ inherently enables grounding via special tags that enclose the grounded noun phrases in \mathbf{G} and segmentation tokens $\mathbf{S} \subset \mathbf{T}_{\text{PRIMA}}$ immediately following \mathbf{G} . The segmentation masks \mathbf{M} are obtained from embedded information in \mathbf{S} us-

ing decoder \mathcal{S} , formalized as $\mathbf{M} = \mathcal{S}(\mathbf{I}, \mathbf{S})$.

3.2. PRIMA Architecture

Our PRIMA architecture, as illustrated in Figure 3, consists of an LVLM backbone and a vision module that incorporates self-supervised semantic features, alongside a segmentation module for pixel grounding.

Large Vision-Language Model \mathcal{L} . To enable multimodal understanding for text generation, we integrate a pretrained Vicuna-7B architecture [9] $\mathcal{L} = \{\mathcal{E}, f_{i-t}\}$ with a vision module \mathcal{E} and an image-to-text projection layer f_{i-t} that aligns visual and text embeddings. The images are first encoded by $\mathcal{E} : \mathbb{R}^{3 \times H \times W} \mapsto \mathbb{R}^{L_I \times D_I}$ to get image embeddings $\mathbf{I}_\mathcal{E} = \mathcal{E}(\mathbf{I}) \in \mathbb{R}^{N_I \times L_I \times D_I}$ with sequence length L_I and hidden size D_I . These embeddings are then passed into $f_{i-t} : \mathbb{R}^{D_I} \mapsto \mathbb{R}^D$ to obtain $\mathbf{I}_{\text{proj}} = f_{i-t}(\mathbf{I}_\mathcal{E})$ in the language model space of hidden size D , which are then interleaved within the embedded text prompt $\mathbf{T}_{\text{embed}} = f_{\mathcal{L} \text{ embed}}(\mathbf{T}_P) \in \mathbb{R}^{L_T \times D}$ to form multimodal embeddings $\mathbf{T} \in \mathbb{R}^{(L_T + N_I \cdot L_I) \times D}$ to be fed into the Vicuna backbone.

In practice, given a text prompt or instruction, we prepend it with a sentence that activates the model’s visual processing, e.g., “The <image> (IMAGE1), <image> (IMAGE2), and <image> (IMAGE3) provide an overview of the pictures,” where each <image> token is replaced with the corresponding projected image embeddings $\mathbf{I}_{\text{proj}} \in \mathbb{R}^{N_I \times L_I \times D}$, and the remaining prompt content is embedded via a standard text embedding layer $f_{\mathcal{L} \text{ embed}}$. The LVLM is trained to generate text that combines reasoning about the question with information necessary for pixel grounding.

Vision Module \mathcal{E} . To enable efficient multi-image understanding, we propose utilizing BLIP-2’s Q-Former cross-attention mechanism [26] to query image representations from visual foundation models. Standard LLaVA-style LVLMs [22, 24, 37] incorporate a CLIP image encoder [35] alongside a simple linear projection layer to bring visual information to the language space. However, this preserves the image embeddings’ sequence lengths, which are often large (e.g., 256 [22] or 576 [37]) and may quickly become expensive as the number of images grows. On the other hand, Q-Former has demonstrated strong results when used in tandem with LVLMs [11], especially in multi-image understanding [25], while having a much shorter sequence length. Therefore, we leverage Q-Former, which uses a set of query tokens alongside an optional text prompt, to extract visual representations from image features before projecting and feeding them into our PRIMA architecture.

Formally, we construct the pre-projection embeddings from \mathbf{I} using our vision module \mathcal{E} , i.e., $\mathbf{I}_\mathcal{E} = \mathcal{E}(\mathbf{I})$. Given image features $\mathbf{I}_\mathcal{V} = \mathcal{V}(\mathbf{I}) \in \mathbb{R}^{N_I \times L_E \times D_E}$ from an image encoder module \mathcal{V} , we employ Q-Former to query efficient embeddings from $\mathbf{I}_\mathcal{V}$, utilizing a set of learnable

query tokens $\mathbf{q} \in \mathbb{R}^{L_q \times D_I}$ and the embedded text $\mathbf{T}_Q = f_{\text{Q-Former embed}}(\mathbf{T}_P) \in \mathbb{R}^{L_Q \times D_I}$. Specifically, we use the concatenation of these embeddings as the query and $\mathbf{I}_\mathcal{V}$ as the and value for Q-Former to fuse representations:

$$\mathbf{I}_\mathcal{E} = \text{Q-Former}(\mathbf{q} \oplus \mathbf{T}_Q, \mathbf{I}_\mathcal{V}) \in \mathbb{R}^{N_I \times L_I \times D_I},$$

where $L_I = L_q + L_Q$ and \oplus denotes concatenation.

Semantic Feature Extractor. To further improve fine-grained object understanding and segmentation, we propose leveraging semantic features from self-supervised Vision Transformers, specifically the DINO series [4, 12, 32]. These features have been shown to contain strong semantic signals useful for object-part understanding, particularly in tasks like semantic correspondence, co-segmentation, and co-part segmentation [2, 59]. To accomplish this, our vision module $\mathcal{V} = \{\text{CLIP}, \text{DINO}, \text{Cross-Attention}\}$ is composed of a Cross-Attention layer to fuse inputs from CLIP and DINO. We first obtain global features from an EVA-CLIP-g/14 model [41] to get $\mathbf{I}_{\text{CLIP}} = \text{CLIP}(\mathbf{I}) \in \mathbb{R}^{N_I \times L_C \times D_C}$. Simultaneously, we also process input images through a pretrained DINOv2-L model with registers [12] to extract semantic features: $\mathbf{I}_{\text{DINO}} = \text{DINO}(\mathbf{I}) \in \mathbb{R}^{N_I \times L_D \times D_D}$. We then employ cross-attention to fuse these features with \mathbf{I}_{CLIP} as the query and \mathbf{I}_{DINO} as the key and value to get:

$$\mathbf{I}_\mathcal{V} = \text{Cross-Attention}(\mathbf{I}_{\text{CLIP}}, \mathbf{I}_{\text{DINO}}) \in \mathbb{R}^{N_I \times L_C \times D_C}.$$

Finally, $\mathbf{I}_\mathcal{V}$ is passed to the Q-Former to obtain image embeddings $\mathbf{I}_\mathcal{E}$, as discussed in the previous section. We finetune the pretrained query tokens \mathbf{q} to imbue them with semantic understanding of the DINOv2 features.

Pixel Grounding. We equip PRIMA with pixel grounding capabilities by incorporating SAM [21], a robust pretrained open-world segmentation model capable of generating segmentation masks from diverse types of input prompts, including text. To leverage this, we follow past works [22, 37] that utilize the LVLM’s text space by training a new token, [SEG], whose final hidden state serves as the prompt for the segmentation model, alongside the encoded images. Consequently, each grounded noun phrase \mathbf{g}_{ji} in the LVLM’s output is paired with its unique [SEG] token. To distinguish tokens associated with different images, we append an image identifier to each segmentation token, e.g., [SEG] (IMAGE2). Finally, to clearly delineate noun phrases within the text output, we train a pair of grounding tokens, <p> and </p>, to enclose each noun phrase. After text generation, we pass the [SEG] tokens, alongside the corresponding SAM-encoded image embeddings, into the finetuned SAM decoder for segmentation.

Formally, from the generated output, we obtain the embeddings $\mathbf{S} = \{\mathbf{S}_1, \dots, \mathbf{S}_{N_I}\}$ of the segmentation tokens [SEG], each $\mathbf{S}_j = \{\mathbf{s}_{j1}, \dots, \mathbf{s}_{jG_j}\} \in \mathbb{R}^{G_j \times D}$ containing the G_j segmentation tokens corresponding to the j -th

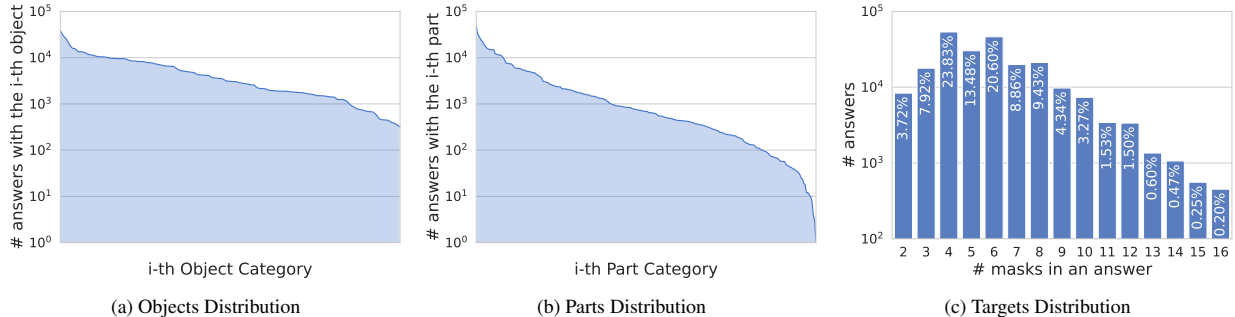


Figure 4. **M⁴SEG distribution plots for (a) objects, (b) parts, and (c) segmentation targets.** Here, (a) and (b) illustrates the frequency of the i -th object and i -th part respectively, sorted by frequency, while (c) shows the percentage of answers containing m masks.

M ⁴ SEG	Train	Test
# QA pairs	224,393	5,000
# Unique objects	115	114
# Unique parts	251	214
Average # object targets per QA	2.74	2.87
Average # part targets per QA	3.09	3.17
Average # total targets per QA	5.83	6.03

Table 2. **M⁴SEG Dataset Summary Statistics.**

image. We then feed these through a text-to-segmentation projection layer $f_{t-s} : \mathbb{R}^D \mapsto \mathbb{R}^{D_S}$ to bring the tokens to the SAM model \mathcal{S} 's encoding space of hidden size D_S and get $\mathbf{S}_{\text{encode}} = f_{t-s}(\mathbf{S})$. We also encode the images \mathbf{I} with \mathcal{S} 's frozen encoder $\mathcal{S}_{\text{encode}} : \mathbb{R}^{3 \times H \times W} \mapsto \mathbb{R}^{D_S}$ to get $\mathbf{I}_{\text{segmentation}} = \mathcal{S}_{\text{encode}}(\mathbf{I})$. Finally, we obtain segmentation masks \mathbf{M} via the finetuned SAM decoder $\mathcal{S}_{\text{decode}}$ by $\mathbf{M} = \mathcal{S}_{\text{decode}}(\mathbf{I}_{\text{segmentation}}, \mathbf{S}_{\text{encode}})$.

Training Objective PRIMA is trained for text generation using a standard next-token prediction cross-entropy loss, denoted as $\mathcal{L}_{\text{text}}$. The segmentation decoder is optimized with a combination of Dice loss ($\mathcal{L}_{\text{Dice}}$) [31] and focal loss ($\mathcal{L}_{\text{focal}}$) [40] as employed in prior works [21, 22, 37]. The overall training objective is defined as $\mathcal{L} = \alpha \mathcal{L}_{\text{text}} + \beta \mathcal{L}_{\text{Dice}} + \gamma \mathcal{L}_{\text{focal}}$, where α , β , and γ are hyperparameters.

4. M⁴SEG Dataset

As summarized in Table 1, existing benchmarks either do not contain part-level information [18, 24, 39], segmentation masks [18, 24] or multiple images [3, 37, 39]. Given the lack of multi-image understanding benchmarks for pixel-grounded reasoning segmentation, we introduce M⁴SEG, a novel dataset that enables the evaluation of large vision-language models on this task. Contrary to previous works, our proposed benchmark has open-set question-answer pairs that incorporate object- and part-level information with corresponding segmentation masks and bounding boxes across multiple images.

Figure 1 presents several examples of our dataset, illustrating the diversity and complexity of comparisons re-

quired at varied reasoning levels. For instance, in the first example, chairs and tables appear in different contexts across three images, with the answer capturing their distinct functions—dining, storage, and workspace—along with the corresponding segmented masks. In another example, our M⁴SEG dataset includes comparisons of objects based on subtle part-level differences, such as variations in the animal and people poses across different images. The open-world nature of examples makes M⁴SEG a challenging reasoning segmentation benchmark that requires complex cross-image visual co-reference, relational reasoning, and grounding at both object and part-level specificities.

Dataset Construction: We utilize three publicly available datasets that contain object- and part-level segmentation masks, ADE20K-Part-234 [49, 65], Pascal-Part [6], and PACO-LVIS [36], to synthesize multi-image comparison question-answer pairs using the GPT-4o API. For each image in these datasets, we sample a set of pairs and triplets of images, ensuring that (1) images represent similar scenes in terms of background or activities, and (2) they contain comparable objects in the scenes that may share some similarity but are not completely identical. We then pass each sampled image set along with their associated bounding box information for the annotated objects and parts to the GPT-4o API and generate question-answer pairs. We ensure that each question requires multi-image reasoning and engages implicit relational understanding, while each answer grounds specific objects and parts across the images. Apart from meticulously designed prompts, we apply a series of filtering steps to further ensure data quality. Specifically, we exclude responses that lack grounding information across multiple images, questions and answers referring to objects or parts not present in the images, and responses involving more than 16 segmentation masks.

The final M⁴SEG data consists of 224k question-answer (QA) pairs. Figure 4 and Table 2 present detailed statistics and distributions of objects, parts, and targets in the dataset. Each QA pair corresponds to an average of 6 targets (objects or parts), with the maximum number in a QA pair reaching

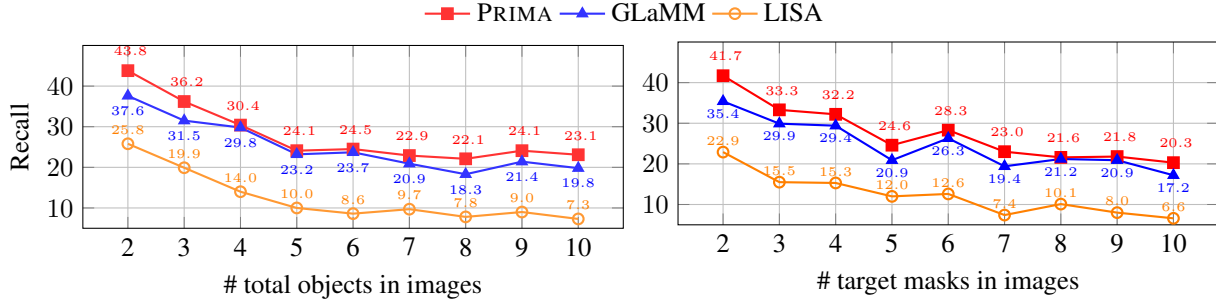


Figure 5. Recall comparison for (a) # objects and (b) # target masks in images.

Model	Segmentation		Reasoning		Computation	
	mIoU \uparrow	Recall \uparrow	SS \uparrow	SIoU \uparrow	TFLOPS \downarrow	Throughput \uparrow
LISA	21.9	10.8	24.5	22.2	88.9	5.20
GLaMM	36.4	22.9	43.2	38.6	83.0	3.37
PRIMA (ours)	38.5	25.0	46.3	42.0	62.0	5.79
Δ Ours - GLaMM	+2.1 \uparrow	+2.1 \uparrow	+3.1 \uparrow	+3.4 \uparrow	-25.3% \downarrow	+71.8% \uparrow

Table 3. **Experimental Results on M⁴SEG.** We report performance metrics for segmentation (mIoU and Recall) and reasoning (Semantic Similarity and S-IoU) to evaluate each model’s ability in multi-image pixel-grounded reasoning segmentation. Computational efficiency metrics (TFLOPs and #samples/sec.) showcase PRIMA’s optimized processing for multi-image tasks.

up to 16. These targets are identified at both object and part levels, making M⁴SEG a valuable resource for advancing models in fine-grained multi-image visual understanding. Additional details are provided in Appendix A.

5. Experiments

To the best of our knowledge, PRIMA is the first model capable of addressing complex coarse to fine-grained pixel reasoning tasks that involve multiple targets across multiple images. To establish baselines, we adapt two state-of-the-art LVLMs, LISA [22] and GLaMM [37] to take multiple images as inputs. Specifically, we append image identifiers (*e.g.*, (IMAGE2)) to the segmentation tokens in the input to differentiate tokens from distinct images, then retrieve image-specific segmentation tokens to generate the corresponding masks using SAM. For a fair comparison, we finetune all three models on M⁴SEG using the same hyperparameters. Each model is fine-tuned for 30 epochs with a batch size of 4, using four A100-40GB GPUs. Following prior works [37, 57], we employ multiple metrics to evaluate the generated segmentation masks and natural language responses, including mIoU, Recall, Semantic Similarity (SS), and S-IoU. Details are provided in Appendix B.

5.1. Experimental Results

Table 3 compares PRIMA against reasoning segmentation baselines. We observe that PRIMA improves both segmentation and reasoning performance. Specifically, in the segmentation-based metrics, PRIMA achieves 2.1 percent-

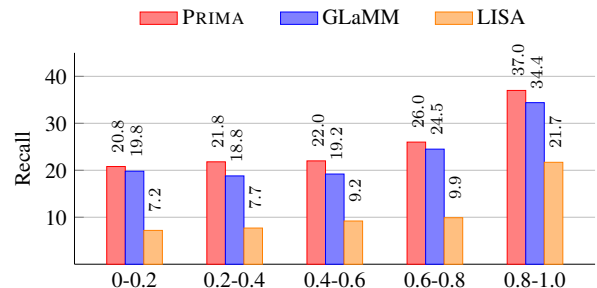


Figure 6. Recall vs. object visibility comparison.

age improvements over the next best baseline. Similarly, for the reasoning metrics, PRIMA improves performance by up to 3.4 percentage points over the next best baseline.

Computational efficiency: Figure 2 and Table 3 highlight the computational efficiency of PRIMA, compared to baselines. PRIMA achieves a notable 25.3% reduction in TFLOPs compared to GLaMM, with a mIoU improvement of 2.1%, indicating that PRIMA not only enhances performance but significantly reduces computational overhead. Additionally, PRIMA uses 10 times fewer tokens than GLaMM, resulting in a throughput relative increase of 71.8% (# samples per second). These results demonstrate the proposed PRIMA model’s optimized design for multi-image pixel-grounded reasoning tasks.

5.2. Ablation Experiments

Number of objects in the images: In Figure 5 (left plot), we observe that models perform worse as the number of objects in the images grows, which indicates that crowded scenes pose a significant challenge. PRIMA consistently outperforms GLaMM in most cases, demonstrating its robustness in handling higher object density.

Number of target masks: In Figure 5 (right plot), we also observe that model performance degrades with the number of target masks in the images, which is expected since it implies a more complex task. Nonetheless, PRIMA consistently outperforms baselines even in more challenging scenarios with a larger number of target masks.

Object visibility: In Figure 6, we observe that model performance improves as the visibility of the objects in input

Q: How do the parts contribute to the structural stability of the stool in the first image and the lamp in the second image?

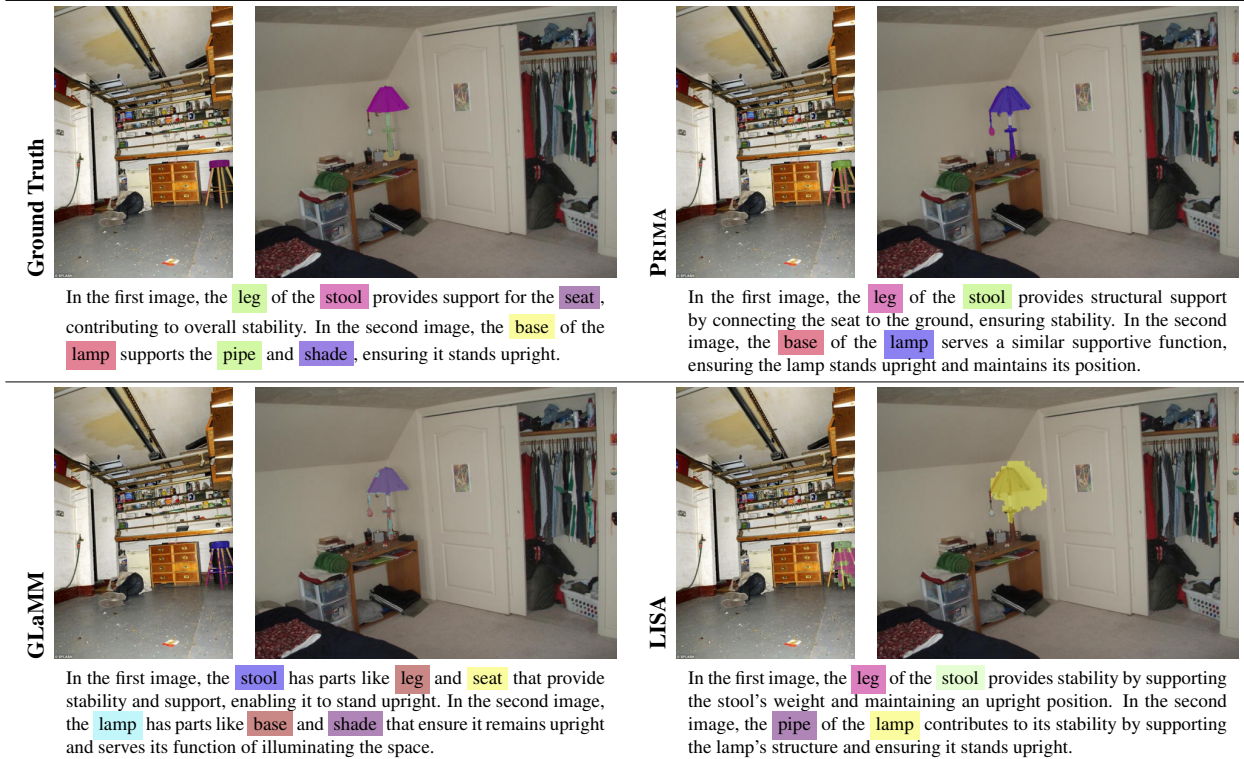


Figure 7. **Qualitative Results.** PRIMA exhibits strong qualitative performance in both segmentation and reasoning, surpassing GLaMM, which shows weak reasoning skills, and LISA, which underperforms in segmentation.

Q-Former	DINOv2	mIoU	Recall	SS	SIoU
✗	✗	36.4	22.9	43.2	38.6
✗	✓	38.5	25.2	47.4	42.9
✓	✗	37.9	25.4	46.2	41.2
✓	✓	38.5	25.0	46.3	42.0

Table 4. **Ablation on PRIMA components.** Both Q-Former and DINOv2 modules enhance PRIMA’s ability to generate high-quality visually grounded responses.

images increases. Object visibility is computed based on the ratio of the object’s mask area to the total image area, weighted by the relative scale disparity among multiple objects within a scene. PRIMA consistently outperforms both GLaMM and LISA across all visibility ranges.

Contribution of the proposed modules: The ablation study in Table 4 demonstrates the individual and combined impact of the Q-Former and DINOv2 modules on PRIMA’s performance. When neither module is used, PRIMA achieves the lowest scores across all metrics, highlighting the necessity of these components for effective grounding and reasoning. Notably, DINOv2 contributes more substantially to fine-grained visual understanding, with a 2.1 and 4.3 percentage increase in mIoU and SIoU due to its inclusion, compared to a 1.5 and 2.6 percentage increase due to Q-Former’s inclusion. While including only

the DINOv2 features without the Q-Former achieves better results in some of the metrics, the absence of the Q-Former module makes the model significantly more expensive computationally. Specifically, PRIMA reduces the number of floating point operations by 37.6% TFLOPS (62.04 vs. 99.29) and increases the throughput by 88.0% samples per second (5.79 vs. 3.08), leading to much faster training and inference time. Therefore, we use Q-Former+DINOv2 as our main model for PRIMA.

5.3. Qualitative Analysis

Figure 7 shows a qualitative comparison between PRIMA, GLaMM, LISA, and Ground Truth data. The top row in the table shows the questions posed to the models, while the corresponding images display the answers and segmentation masks generated by each model, alongside the Ground Truth reference. For clarity, we use the same colors for segmentation masks as the highlighted text corresponding to the object/part. Results demonstrate that PRIMA outperforms both baselines in segmentation tasks, while also providing more accurate answers. In contrast, GLaMM and LISA confuse the reasoning for the stability of the stool and lamp, respectively, while LISA demonstrates slightly better reasoning than GLaMM.

6. Conclusion

In this work, we introduce the new task of multi-image pixel-grounded reasoning segmentation. To support training and evaluation, we release the M⁴SEG benchmark, laying the foundation for future research in multi-image pixel-grounding LVLMs. Finally, we propose PRIMA, a novel vision-language reasoning segmentation model that combines pixel-level grounding with multi-image reasoning capabilities. Experimental results demonstrate PRIMA’s superior performance and efficiency over SoTA baselines. We hope this work encourages future vision-language applications in real-world, complex reasoning tasks.

Acknowledgments

This research is based upon work partially supported by U.S. DARPA ECOLE Program No. HR00112390062. The views and conclusions contained herein are those of the authors and should not be interpreted as necessarily representing the official policies, either expressed or implied, of DARPA or the U.S. Government. The U.S. Government is authorized to reproduce and distribute reprints for governmental purposes notwithstanding any copyright annotation therein.

References

- [1] Alayrac, Jean-Baptiste and Donahue, Jeff and Luc, Pauline and Miech, Antoine and Barr, Iain and Hasson, Yana and Lenc, Karel and Mensch, Arthur and Millican, Katherine and Reynolds, Malcolm and others. Flamingo: a Visual Language Model for Few-Shot Learning. In *Conference on Neural Information Processing Systems*, 2022. 3
- [2] Amir, Shir and Gandelsman, Yossi and Bagon, Shai and Dekel, Tali. Deep ViT Features as Dense Visual Descriptors. In *ECCVW What is Motion For?*, 2022. 5
- [3] Anonymous. MMR: A Large-scale Benchmark Dataset for Multi-target and Multi-granularity Reasoning Segmentation. *Submitted to the International Conference on Learning Representations*, 2025. Under review. 3, 6
- [4] Caron, Mathilde and Touvron, Hugo and Misra, Ishan and Jégou, Hervé and Mairal, Julien and Bojanowski, Piotr and Joulin, Armand. Emerging Properties in Self-Supervised Vision Transformers. In *International Conference on Computer Vision*, 2021. 5
- [5] Chen, Keqin and Zhang, Zhao and Zeng, Weili and Zhang, Richong and Zhu, Feng and Zhao, Rui. Shikra: Unleashing Multimodal LLM’s Referential Dialogue Magic. *arXiv preprint arXiv:2306.15195*, 2023. 3
- [6] Chen, Xianjie and Mottaghi, Roozbeh and Liu, Xiaobai and Fidler, Sanja and Urtasun, Raquel and Yuille, Alan. Detect What You Can: Detecting and Representing Objects using Holistic Models and Body Parts. In *IEEE/CVF Conference on Computer Vision and Pattern Recognition*, 2014. 6, 1
- [7] Chen, Yen-Chun and Li, Linjie and Yu, Licheng and El Kholly, Ahmed and Ahmed, Faisal and Gan, Zhe and Cheng, Yu and Liu, Jingjing. UNITER: UNiversal Image-Text Representation Learning. In *European Conference on Computer Vision*, 2020. 2
- [8] Cheng, Tianheng and Song, Lin and Ge, Yixiao and Liu, Wenyu and Wang, Xinggang and Shan, Ying. YOLO-World: Real-Time Open-Vocabulary Object Detection. In *IEEE/CVF Conference on Computer Vision and Pattern Recognition*, 2024. 2
- [9] Chiang, Wei-Lin and Li, Zhuohan and Lin, Zi and Sheng, Ying and Wu, Zhanghao and Zhang, Hao and Zheng, Lianmin and Zhuang, Siyuan and Zhuang, Yonghao and Gonzalez, Joseph E. and Stoica, Ion and Xing, Eric P. Vicuna: An Open-Source Chatbot Impressing GPT-4 with 90%* ChatGPT Quality, 2023. 5
- [10] Conti, Alessandro and Fini, Enrico and Mancini, Massimiliano and Rota, Paolo and Wang, Yiming and Ricci, Elisa. Vocabulary-free Image Classification. In *Conference on Neural Information Processing Systems*, 2023. 2
- [11] Dai, Wenliang and Li, Junnan and Li, Dongxu and Tiong, Anthony Meng Huat and Zhao, Junqi and Wang, Weisheng and Li, Boyang and Fung, Pascale and Hoi, Steven. Instruct-BLIP: Towards General-purpose Vision-Language Models with Instruction Tuning. In *Conference on Neural Information Processing Systems*, 2023. 5
- [12] Darcet, Timothée and Oquab, Maxime and Mairal, Julien and Bojanowski, Piotr. Vision Transformers Need Registers. In *International Conference on Learning Representations*, 2024. 5
- [13] Deng, Yihe and Lu, Pan and Yin, Fan and Hu, Ziniu and Shen, Sheng and Zou, James and Chang, Kai-Wei and Wang, Wei. Enhancing Large Vision Language Models with Self-Training on Image Comprehension. *arXiv preprint arXiv:2405.19716*, 2024. 3
- [14] Dong, Runpei and Han, Chunrui and Peng, Yuang and Qi, Zekun and Ge, Zheng and Yang, Jinrong and Zhao, Liang and Sun, Jianjian and Zhou, Hongyu and Wei, Haoran and others. DreamLLM: Synergistic Multimodal Comprehension and Creation. In *International Conference on Learning Representations*, 2024. 3
- [15] Guo, Qiushan and De Mello, Shalini and Yin, Hongxu and Byeon, Wonmin and Cheung, Ka Chun and Yu, Yizhou and Luo, Ping and Liu, Sifei. RegionGPT: Towards Region Understanding Vision Language Model. In *IEEE/CVF Conference on Computer Vision and Pattern Recognition*, 2024. 3
- [16] Huang, Yupan and Meng, Zaiqiao and Liu, Fangyu and Su, Yixuan and Collier, Nigel and Lu, Yutong. Sparkles: Unlocking Chats Across Multiple Images for Multimodal Instruction-Following Models. In *ICLR Workshop on Navigating and Addressing Data Problems for Foundation Models*, 2024. 2, 3
- [17] Jia, Mengzhao and Yu, Wenhao and Ma, Kaixin and Fang, Tianqing and Zhang, Zhihan and Ouyang, Siru and Zhang, Hongming and Jiang, Meng and Yu, Dong. LEOPARD: A Vision Language Model For Text-Rich Multi-Image Tasks. *arXiv preprint arXiv:2410.01744*, 2024. 3
- [18] Jiang, Dongfu and He, Xuan and Zeng, Huaye and Wei, Cong and Ku, Max and Liu, Qian and Chen, Wenhui. MAN-

- TIS: Interleaved Multi-Image Instruction Tuning. *arXiv preprint arXiv:2405.01483*, 2024. 3, 6
- [19] Kar, Oğuzhan Fatih and Tonioni, Alessio and Poklukar, Petra and Kulshrestha, Achin and Zamir, Amir and Tombari, Federico. BRAVE: Broadening the visual encoding of vision-language models. In *European Conference on Computer Vision*, 2025. 4
- [20] Kil, Jihyung and Mai, Zheda and Lee, Justin and Wang, Zihe and Cheng, Kerrie and Wang, Lemeng and Liu, Ye and Chowdhury, Arpita and Chao, Wei-Lun. CompBench: A Comparative Reasoning Benchmark for Multimodal LLMs. In *Conference on Neural Information Processing Systems*, 2024. 3
- [21] Kirillov, Alexander and Mintun, Eric and Ravi, Nikhila and Mao, Hanzi and Rolland, Chloe and Gustafson, Laura and Xiao, Tete and Whitehead, Spencer and Berg, Alexander C and Lo, Wan-Yen and others. Segment Anything. In *International Conference on Computer Vision*, 2023. 5, 6, 1
- [22] Lai, Xin and Tian, Zhuotao and Chen, Yukang and Li, Yanwei and Yuan, Yuhui and Liu, Shu and Jia, Jiaya. LISA: Reasoning Segmentation via Large Language Model. In *IEEE/CVF Conference on Computer Vision and Pattern Recognition*, 2024. 2, 3, 4, 5, 6, 7
- [23] Li, Feng and Zhang, Hao and Sun, Peize and Zou, Xueyan and Liu, Shilong and Yang, Jianwei and Li, Chunyuan and Zhang, Lei and Gao, Jianfeng. Semantic-SAM: Segment and Recognize Anything at Any Granularity. In *European Conference on Computer Vision*, 2024. 2
- [24] Li, Feng and Zhang, Renrui and Zhang, Hao and Zhang, Yuanhan and Li, Bo and Li, Wei and Ma, Zejun and Li, Chunyuan. LLaVA-NeXT-Interleave: Tackling Multi-image, Video, and 3D in Large Multimodal Models. *arXiv preprint arXiv:2407.07895*, 2024. 3, 5, 6
- [25] Li, Juncheng and Pan, Kaihang and Ge, Zhiqi and Gao, Minghe and Ji, Wei and Zhang, Wenqiao and Chua, Tat-Seng and Tang, Siliang and Zhang, Hanwang and Zhuang, Yueting. Fine-tuning Multimodal LLMs to Follow Zero-shot Demonstrative Instructions. In *International Conference on Learning Representations*, 2023. 2, 3, 5
- [26] Li, Junnan and Li, Dongxu and Savarese, Silvio and Hoi, Steven. BLIP-2: Bootstrapping Language-Image Pre-training with Frozen Image Encoders and Large Language Models. In *International Conference on Machine Learning*, 2023. 2, 3, 5
- [27] Li, Yanwei and Zhang, Yuechen and Wang, Chengyao and Zhong, Zhisheng and Chen, Yixin and Chu, Ruihang and Liu, Shaoteng and Jia, Jiaya. Mini-Gemini: Mining the Potential of Multi-modality Vision Language Models. *arXiv preprint arXiv:2403.18814*, 2024. 4
- [28] Lin, Wei and Mirza, Muhammad Jehanzeb and Doveh, Sivan and Feris, Rogerio and Giryes, Raja and Hochreiter, Sepp and Karlinsky, Leonid. Comparison Visual Instruction Tuning. *arXiv preprint arXiv:2406.09240*, 2024. 3
- [29] Liu, Haotian and Li, Chunyuan and Wu, Qingyang and Lee, Yong Jae. Visual Instruction Tuning. In *Conference on Neural Information Processing Systems*, 2024. 2, 3
- [30] Ma, Chuofan and Jiang, Yi and Wu, Jiannan and Yuan, Zehuan and Qi, Xiaojuan. Groma: Localized Visual Tokenization for Grounding Multimodal Large Language Models. In *European Conference on Computer Vision*, 2025. 3
- [31] Milletari, Fausto and Navab, Nassir and Ahmadi, Seyed-Ahmad. V-Net: Fully Convolutional Neural Networks for Volumetric Medical Image Segmentation. In *International Conference on 3D Vision (3DV)*, 2016. 6
- [32] Oquab, Maxime and Darcet, Timothée and Moutakanni, Théo and Vo, Huy V and Szafraniec, Marc and Khaldov, Vasil and Fernandez, Pierre and HAZIZA, Daniel and Massa, Francisco and El-Nouby, Alaaeldin and others. DINOv2: Learning Robust Visual Features without Supervision. *Transactions on Machine Learning Research*, 2024. 5, 1
- [33] Peng, Zhiliang and Wang, Wenhui and Dong, Li and Hao, Yaru and Huang, Shaohan and Ma, Shuming and Wei, Furu. Grounding Multimodal Large Language Models to the World. In *International Conference on Learning Representations*, 2024. 3
- [34] Qu, Xiaoye and Sun, Jiashuo and Wei, Wei and Cheng, Yu. Look, Compare, Decide: Alleviating Hallucination in Large Vision-Language Models via Multi-View Multi-Path Reasoning. *arXiv preprint arXiv:2408.17150*, 2024. 3
- [35] Radford, Alec and Kim, Jong Wook and Hallacy, Chris and Ramesh, Aditya and Goh, Gabriel and Agarwal, Sandhini and Sastry, Girish and Askell, Amanda and Mishkin, Pamela and Clark, Jack and others. Learning Transferable Visual Models From Natural Language Supervision. In *International Conference on Machine Learning*, 2021. 5
- [36] Ramanathan, Vignesh and Kalia, Anmol and Petrovic, Vladan and Wen, Yi and Zheng, Baixue and Guo, Baishan and Wang, Rui and Marquez, Aaron and Kovvuri, Rama and Kadian, Abhishek and others. PACO: Parts and Attributes of Common Objects. In *IEEE/CVF Conference on Computer Vision and Pattern Recognition*, 2023. 6, 1
- [37] Rasheed, Hanoona and Maaz, Muhammad and Shaji, Sahal and Shaker, Abdelrahman and Khan, Salman and Cholakkal, Hisham and Anwer, Rao M and Xing, Eric and Yang, Ming-Hsuan and Khan, Fahad S. GLaMM: Pixel Grounding Large Multimodal Model. In *IEEE/CVF Conference on Computer Vision and Pattern Recognition*, 2024. 2, 3, 4, 5, 6, 7, 1
- [38] Reimers, Nils and Gurevych, Iryna. Sentence-BERT: Sentence Embeddings using Siamese BERT-Networks. In *Empirical Methods in Natural Language Processing and International Joint Conference on Natural Language Processing*, 2019. 2
- [39] Ren, Zhongwei and Huang, Zhicheng and Wei, Yunchao and Zhao, Yao and Fu, Dongmei and Feng, Jiashi and Jin, Xiaojie. PixelLM: Pixel Reasoning with Large Multimodal Model. In *IEEE/CVF Conference on Computer Vision and Pattern Recognition*, 2024. 3, 4, 6
- [40] Ross, T-YLPG and Dollár, GKHP. Focal Loss for Dense Object Detection. In *IEEE/CVF Conference on Computer Vision and Pattern Recognition*, 2017. 6
- [41] Sun, Quan and Fang, Yuxin and Wu, Ledell and Wang, Xinlong and Cao, Yue. EVA-CLIP: Improved Training Techniques for CLIP at Scale. *arXiv preprint arXiv:2303.15389*, 2023. 5

- [42] Sun, Quan and Yu, Qiyang and Cui, Yufeng and Zhang, Fan and Zhang, Xiaosong and Wang, Yueze and Gao, Hongcheng and Liu, Jingjing and Huang, Tiejun and Wang, Xinlong. Emu: Generative Pretraining in Multimodality. In *International Conference on Learning Representations*, 2023. 3
- [43] Wang, Junchi and Ke, Lei. LLM-Seg: Bridging Image Segmentation and Large Language Model Reasoning. In *IEEE/CVF Conference on Computer Vision and Pattern Recognition*, 2024. 3
- [44] Wang, Peng and Yang, An and Men, Rui and Lin, Junyang and Bai, Shuai and Li, Zhikang and Ma, Jianxin and Zhou, Chang and Zhou, Jingren and Yang, Hongxia. OFA: Unifying Architectures, Tasks, and Modalities Through a Simple Sequence-to-Sequence Learning Framework. In *International Conference on Machine Learning*, 2022. 2
- [45] Wang, Weihang and Lv, Qingsong and Yu, Wenmeng and Hong, Wenyi and Qi, Ji and Wang, Yan and Ji, Junhui and Yang, Zhuoyi and Zhao, Lei and Song, Xixuan and others. CogVLM: Visual Expert for Pretrained Language Models. In *Conference on Neural Information Processing Systems*, 2024. 3
- [46] Wang, Weiyun and Shi, Min and Li, Qingyun and Wang, Wenhao and Huang, Zhenhang and Xing, Linjie and Chen, Zhe and Li, Hao and Zhu, Xizhou and Cao, Zhiguo and others. The All-Seeing Project: Towards Panoptic Visual Recognition and Understanding of the Open World. In *International Conference on Learning Representations*, 2024. 3
- [47] Wang, Wenxuan and Yue, Tongtian and Zhang, Yisi and Guo, Longteng and He, Xingjian and Wang, Xinlong and Liu, Jing. Unveiling Parts Beyond Objects: Towards Finer-Granularity Referring Expression Segmentation. In *IEEE/CVF Conference on Computer Vision and Pattern Recognition*, 2024. 3
- [48] Wang, Xidong and Song, Dingjie and Chen, Shunian and Zhang, Chen and Wang, Benyou. LongLLaVA: Scaling Multi-modal LLMs to 1000 Images Efficiently via Hybrid Architecture. *arXiv preprint arXiv:2409.02889*, 2024. 3
- [49] Wei, Meng and Yue, Xiaoyu and Zhang, Wenwei and Kong, Shu and Liu, Xihui and Pang, Jiangmiao. OV-PARTS: Towards Open-Vocabulary Part Segmentation. In *Conference on Neural Information Processing Systems*, 2024. 6, 1
- [50] Wu, Siwei and Zhu, Kang and Bai, Yu and Liang, Yiming and Li, Yizhi and Wu, Haoning and Liu, Jiaheng and Liu, Ruibo and Qu, Xingwei and Cheng, Xuxin and others. MMRA: A Benchmark for Evaluating Multi-Granularity and Multi-Image Relational Association Capabilities in Large Visual Language Models. *arXiv preprint arXiv:2407.17379*, 2024. 3
- [51] Wu, Tsung-Han and Biamby, Giscard and Chan, David and Dunlap, Lisa and Gupta, Ritwik and Wang, Xudong and Gonzalez, Joseph E and Darrell, Trevor. See Say and Segment: Teaching LLMs to Overcome False Premises. In *IEEE/CVF Conference on Computer Vision and Pattern Recognition*, 2024. 3
- [52] Yan, Siming and Bai, Min and Chen, Weifeng and Zhou, Xiong and Huang, Qixing and Li, Erran. ViGoR: Improving Visual Grounding of Large Vision Language Models with Fine-Grained Reward Modeling. In *European Conference on Computer Vision*, 2024. 3
- [53] Yang, Senqiao and Qu, Tianyuan and Lai, Xin and Tian, Zhuotao and Peng, Bohao and Liu, Shu and Jia, Jiaya. LISA++: An Improved Baseline for Reasoning Segmentation with Large Language Model. *arXiv e-prints*, 2023. 4
- [54] Ye, Jiabo and Xu, Haiyang and Liu, Haowei and Hu, Anwen and Yan, Ming and Qian, Qi and Zhang, Ji and Huang, Fei and Zhou, Jingren. mPLUG-Owl3: Towards Long Image-Sequence Understanding in Multi-Modal Large Language Models. *arXiv preprint arXiv:2408.04840*, 2024. 3
- [55] You, Haoxuan and Zhang, Haotian and Gan, Zhe and Du, Xianzhi and Zhang, Bowen and Wang, Zirui and Cao, Liangliang and Chang, Shih-Fu and Yang, Yinfei. Ferret: Refer and Ground Anything Anywhere at Any Granularity. In *International Conference on Learning Representations*, 2024. 3
- [56] You, Haoxuan and Zhang, Haotian and Gan, Zhe and Du, Xianzhi and Zhang, Bowen and Wang, Zirui and Cao, Liangliang and Chang, Shih-Fu and Yang, Yinfei. Ferret: Refer and Ground Anything Anywhere at Any Granularity. In *International Conference on Learning Representations*, 2024. 3
- [57] Yuan, Yuqian and Li, Wentong and Liu, Jian and Tang, Dongqi and Luo, Xinjie and Qin, Chi and Zhang, Lei and Zhu, Jianke. Osprey: Pixel Understanding with Visual Instruction Tuning. In *IEEE/CVF Conference on Computer Vision and Pattern Recognition*, 2024. 3, 7, 2
- [58] Zhang, Ao and Zhao, Liming and Xie, Chen-Wei and Zheng, Yun and Ji, Wei and Chua, Tat-Seng. NExT-Chat: An LMM for Chat, Detection and Segmentation. In *International Conference on Machine Learning*, 2024. 4
- [59] Zhang, Junyi and Herrmann, Charles and Hur, Junhwa and Polania Cabrera, Luisa and Jampani, Varun and Sun, Deqing and Yang, Ming-Hsuan. A Tale of Two Features: Stable Diffusion Complements DINO for Zero-Shot Semantic Correspondence. In *Conference on Neural Information Processing Systems*, 2024. 5
- [60] Zhang, Shilong and Sun, Peize and Chen, Shoufa and Xiao, Min and Shao, Wenqi and Zhang, Wenwei and Liu, Yu and Chen, Kai and Luo, Ping. GPT4RoI: Instruction Tuning Large Language Model on Region-of-Interest. *arXiv preprint arXiv:2307.03601*, 2023. 3
- [61] Zhang, Tao and Li, Xiangtai and Fei, Hao and Yuan, Haobo and Wu, Shengqiong and Ji, Shunping and Loy, Chen Change and Shuicheng, YAN. OMG-LLaVA: Bridging Image-level, Object-level, Pixel-level Reasoning and Understanding. In *Conference on Neural Information Processing Systems*, 2024. 4
- [62] Zhang, Yichi and Ma, Ziqiao and Gao, Xiaofeng and Shakhia, Suhaila and Gao, Qiaozhi and Chai, Joyce. GROUNDHOG: Grounding Large Language Models to Holistic Segmentation. In *IEEE/CVF Conference on Computer Vision and Pattern Recognition*, 2024. 4
- [63] Zhang, Zheng and Ma, Yeyao and Zhang, Enming and Bai, Xiang. PSALM: Pixelwise Segmentation with Large Multi-

- Modal Model. In *European Conference on Computer Vision*, 2025. 4
- [64] Zhang, Zhuosheng and Zhang, Aston and Li, Mu and Zhao, Hai and Karypis, George and Smola, Alex. Multimodal Chain-of-Thought Reasoning in Language Models. *Transactions on Machine Learning Research*, 2024. 3
- [65] Zhou, Bolei and Zhao, Hang and Puig, Xavier and Fidler, Sanja and Barriuso, Adela and Torralba, Antonio. Scene Parsing through ADE20K Dataset. In *IEEE/CVF Conference on Computer Vision and Pattern Recognition*, 2017. 6, 1
- [66] Zhou, Li and Yuan, Xu and Sun, Zenghui and Zhou, Zikun and Lan, Jingsong. Instruction-guided Multi-Granularity Segmentation and Captioning with Large Multimodal Model. *arXiv preprint arXiv:2409.13407*, 2024. 3
- [67] Zhou, Yucheng and Li, Xiang and Wang, Qianning and Shen, Jianbing. Visual In-Context Learning for Large Vision-Language Models. In *Findings of the Association for Computational Linguistics*, 2024. 3
- [68] Zolkepli, Husein and Razak, Aisyah and Adha, Kamarul and Nazhan, Ariff. MMMModal–Multi-Images Multi-Audio Multi-turn Multi-Modal. *arXiv preprint arXiv:2402.11297*, 2024. 3



PRIMA: Multi-Image Vision-Language Models for Reasoning Segmentation

Supplementary Material

A. M⁴SEG Dataset Construction

A.1. Seed Datasets

- **ADE20K-Part-234** [49, 65]: The ADE20K-Part-234 dataset [49] provides part-level annotations of 44 objects and 234 parts, derived from the widely used SceneParse150 subset of the ADE20K [65] dataset by selecting the objects with more than one frequently annotated part and merging duplicated parts.
- **Pascal-Part** [6]: The PASCAL-Part dataset is an enhanced PASCAL VOC 2010 [6] dataset by adding segmentation masks for each object’s body parts and silhouette annotations for categories without consistent parts.
- **PACO-LVIS** [36]: PACO-LVIS [36] is a detection dataset derived from LVIS images, providing rich annotations, including part masks, object categories, object-part categories, and attributes, for 75 object classes.

A.2. Dataset Sampling

Feature Extraction. To find similar images, we first extract DINOv2 [32] features $\text{DINO}(\mathbf{I}_i)$ corresponding to each image sample \mathbf{I}_i . We then define the distance between two image samples \mathbf{I}_i and \mathbf{I}_j using the cosine distance

$$d(\mathbf{I}_i, \mathbf{I}_j) = 1 - \frac{\text{DINO}(\mathbf{I}_i) \cdot \text{DINO}(\mathbf{I}_j)}{\|\text{DINO}(\mathbf{I}_i)\| \cdot \|\text{DINO}(\mathbf{I}_j)\|}. \quad (1)$$

To ensure the diversity and relevance of the image sets in the dataset, for each image, we sample a set containing 2 or 3 related images according to the following two criteria:

Nearest Neighbor Sampling: For each image in the dataset, we sample $n = \{1, 2\}$ images from its k -nearest neighbors, where k is empirically set to 20. This ensures that the M⁴SEG dataset contains image sets that compare objects and parts in similar scenes.

Object-Category based Sampling: We also manually annotate all possible object pairs across the three datasets by evaluating whether comparisons between objects from given categories are meaningful. For each object, we then sample all images containing at least one occurrence of that object. Next, we filter images containing objects from relevant categories and randomly sample $n = \{2, 3\}$ images from the remaining k_2 -nearest neighbors, where k_2 is empirically set to 5. This criterion ensures that the M⁴SEG dataset consists of image sets that compare objects and parts that are closely related.

A.3. Question-Answer Pair Generation

We use the GPT-4o API (gpt-4o-2024-08-06) to generate question-answer pairs for the sampled image sets. We employ a temperature of 1.0 to maintain a balance between correctness and diversity. We carefully design a prompt to generate 3-5 question-answer pairs per image set.

To ensure precise identification and referencing, in each prompt, we provide the GPT-4o model with a complete list of all the objects and parts, along with their associated bounding-box information. To distinguish multiple instances of the same object or part, we append unique identifiers to their names in the format NAME.XYY for objects and NAME.XYYZZ for parts. Here, the first digit X denotes the image the annotation belongs to. The next two digits YY provide a unique identifier for the object within that image. Similarly, the last two digits ZZ denote a unique identifier for the part in that image. These identifiers are later used to extract the corresponding grounding information during data preprocessing.

A.4. Dataset Filtering

Despite careful curation of image sets and prompts, the GPT-4o API occasionally produces erroneous question-answer pairs due to hallucinations, instruction-following errors, and related issues. Consequently, to ensure the quality of the M⁴SEG dataset, we implement a robust filtering strategy to eliminate faulty question-answer pairs. Specifically: (a) we discard questions that merely list objects or parts in the images without grounding; (b) we filter out questions referencing locations as bounding boxes; (c) we filter pairs where answers do not encompass all provided images; (d) we retain only pairs where answers include at least one segmentation mask from each of the images; and (e) we exclude pairs mentioning objects or parts not present in the images. This process discards 38,873 question-answer pairs (14.74% of the dataset).

B. Evaluation Metrics

Mean Intersection over Union (mIoU) [21]: mIoU is a key metric to determine how accurately the model is predicting the segmentation boundaries by providing the average overlap between the predicted segmentation masks and the ground truth masks across all classes.

Recall [37]: Recall is a metric that reflects the model’s ability to capture all relevant instances by measuring the ratio of true positive instances correctly identified by a

model from all the actual positive instances. In particular, we follow recent work [37] to obtain true positives by (1) identifying predictions with IoU values higher than a threshold of 0.5, and, of these, (2) choosing the prediction with the highest IoU that also has a SentenceBERT [38] semantic similarity score over a 0.5 threshold, qualifying it as a text-mask match, *i.e.*, a true positive.

SS [10]: Following past works [10, 57], we compute semantic Similarity (SS) as the similarity between predicted and ground truth labels in the SentenceBERT [38] embedding space.

S-IoU [10]: Semantic IoU (SIoU) is the word overlap between predicted and ground truth labels.

C. Implementation Details

We implement and optimize PRIMA using PyTorch, specifically DeepSpeed for efficient parallel training. Our model is initialized with the GLaMM [37] checkpoint¹ and trained on four NVIDIA A100 GPUs with 40GBs of memory for 30 epochs, each with 500 steps. LoRA layers are used on attention queries and keys within the LLM and set with rank 8 and a scaling factor of 16. We leverage the AdamW optimizer with an initial learning rate of 3e-4 and beta coefficients of 0.9 and 0.95. We train PRIMA with a batch size of 4 and a gradient accumulation step size of 2.

D. Low Tail Analysis

In this experiment, we study the effect of object and part frequency on PRIMA’s performance. In Figure 8 (a) and (b), we observe that both objects and parts in the M⁴SEG dataset have a low-tailed distribution, where less frequent object and part categories exhibit significantly fewer examples, leading to class imbalance challenges. However, in Figure 8 (c) and (d), we observe there is no clear pattern in PRIMA’s performance against either object or part frequency. This shows that PRIMA is robust to the low-tailed distribution and does not overfit to more frequent categories.

E. PRIMA in the wild

We additionally provide examples of images collected from the web that PRIMA has not seen during training. In Figure 9, we observe that PRIMA demonstrates strong generalization to these unseen images.

¹<https://huggingface.co/MBZUAI/GLaMM-FullScope>.

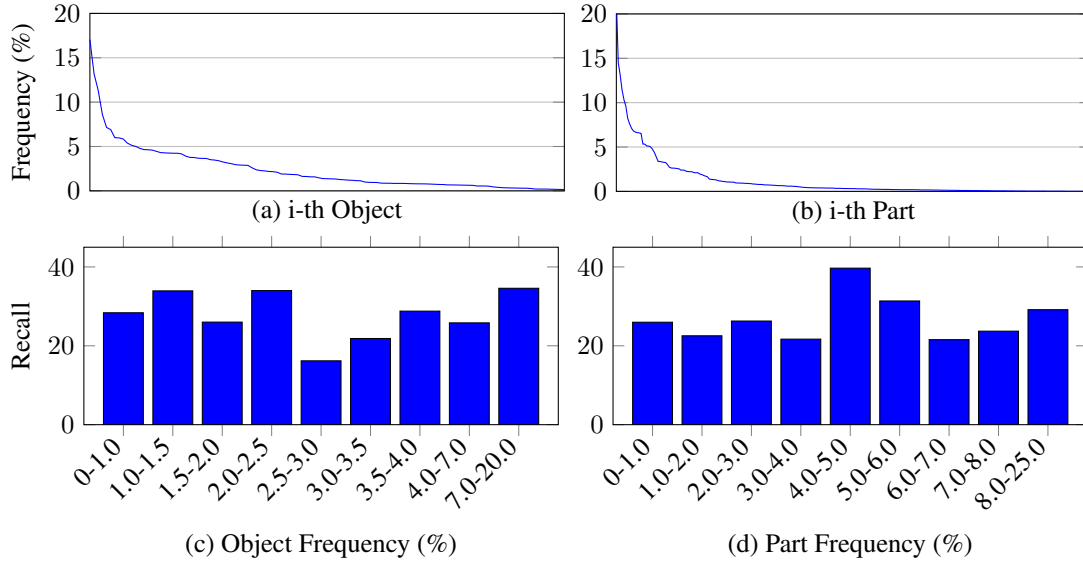


Figure 8. **Low-tail analysis of objects and parts in M^4SEG .** (a) and (b) denote the frequency of the objects and parts, demonstrating a low-tail distribution. (c) and (d) shows PRIMA’s performance across varying object and part frequency levels.

			
Q: What can I use to have a dinner with my family?		Q: What can I use to cut a piece of paper and why?	
A: The table [SEG] from Image 1, which includes parts like table's top [SEG] and table's leg [SEG], to set up a dinner for the family. The table's size and structure are suitable for accommodating multiple plates and serving dishes.		A: Scissor [SEG] in Image 2 can be used to cut a piece of paper. This is because the scissors's blade [SEG] and scissors's handle [SEG] provide the necessary cutting power and grip for cutting paper.	
			
Q: Which one can carry more people?		Q: Which one is more comfortable to sit on?	
A: The bus [SEG] in Image 1 can carry more people due to its larger body, as seen in bus's body [SEG], compared to car [SEG] in Image 2 with car's body [SEG], which is smaller.		A: The armchair [SEG] in Image 1 is more comfortable to sit on due to its seat base [SEG] and seat [SEG], which provide a supportive and cushioned seating surface. In contrast, the bench [SEG] in Image 2 lacks such cushioning and might be less comfortable for prolonged sitting.	

Figure 9. **PRIMA in the wild.** Example questions and responses demonstrating PRIMA’s ability to ground multi-image reasoning at a fine-grained part level on images from the web. For conciseness, we visualize only a few of the segmentation masks [SEG] from the ones PRIMA generates for these images.